Current Drive Experiments in the HIT-II Spherical Tokamak

T. R. Jarboe, P. Gu, V. A. Izzo, P. E. Jewell, K. J. McCollam, B. A. Nelson, R. Raman, A. J. Redd, P. E. Sieck, and R. J. Smith, *Aerospace & Energetics Research Program, University of Washington, Seattle, Washington, USA,*

M. Nagata, T. Uyama, *Himeji Institute of Technology, Himeji, Japan*

e-mail: Jarboe@aa.washington.edu

Abstract. The Helicity Injected Torus (HIT) program has made progress in understanding relaxation and helicity injection current drive. Helicity-conserving MHD activity during the inductive (Ohmic) current ramp demonstrates the profile flattening needed for coaxial helicity injection (CHI). Results from cathode and anode central column (CC) CHI pulses are consistent with the electron locking model of current drive from a pure *n=1* mode. Finally, low density CHI, compatible with Ohmic operation, has been achieved. Some enhancement of CHI discharges with the application of Ohmic is shown.

1. Introduction

The purpose of the HIT program is to study and develop helicity injection current drive for magnetic confinement [1-3]. A fusion reactor requires an efficient method of steady-state current drive. Current drive methods involving neutral beams and radio frequency waves have efficiencies as low as 0.1% when scaled to a reactor [4,5]. Current drive by CHI has predicted reactor efficiencies in the tens of percent [1] reducing the dominance of the cost of current drive in a reactor to insignificance. The HIT experiment was motivated by the success of CHI current drive on spheromaks [6] and by helicity injection current drive on reversed field pinches [7] and tokamaks [8]. The first HIT experiment was a low aspect ratio tokamak with major radius 0.3 m, minor radius 0.2 m, and elongation 1.75. Only CHI was used to form and sustain the tokamak where currents as high as 250 kA and electron temperatures as high as 100 eV were achieved at densities of $3\text{-}10\text{x}10^{19}$ m^{-3}. External equilibrium and stability currents were provided passively by a 10 mm thick copper shell flux conserver. The results reported here are from the HIT-II experiment, which has the same basic geometry as HIT. The 10 mm thick copper outer shell and 12 mm thick copper central conductor of HIT are replaced by a 6 mm thick 304 stainless steel shell (L/R=1.2ms) and a 3.5 mm thick 304 stainless steel central conductor. The central conductor is covered with a 12 mm thick graphite [Union Carbide type ATJ] cylinder. A feedback controlled coil set provides equilibrium fields and also transformer action [3].

2. MHD activity in Ohmic discharges

The study of Ohmic plasmas in the HIT-II Spherical Tokamak (ST) has provided useful comparisons, both with CHI results from HIT-II and with Ohmic plasma results from other ST experiments [9]. The Ohmic plasmas in HIT-II exhibit MHD events during both the current ramp-up and current decay. These events are characterized by low mode number precursors (typically n=1), a significant loss of plasma, and changes to the MHD equilibrium. Figure 1 shows the activity on the current rise that may be analogous to the double tearing mode seen on a normal tokamak with a high current ramp rate. The plasma current is measured using Rogowski segments around the poloidal perimeter outside the vacuum shell. The vessel currents due to transformer action are subtracted. However, the eddy currents in the shell produced by the event are not corrected. Thus, these Rogowski segments have a

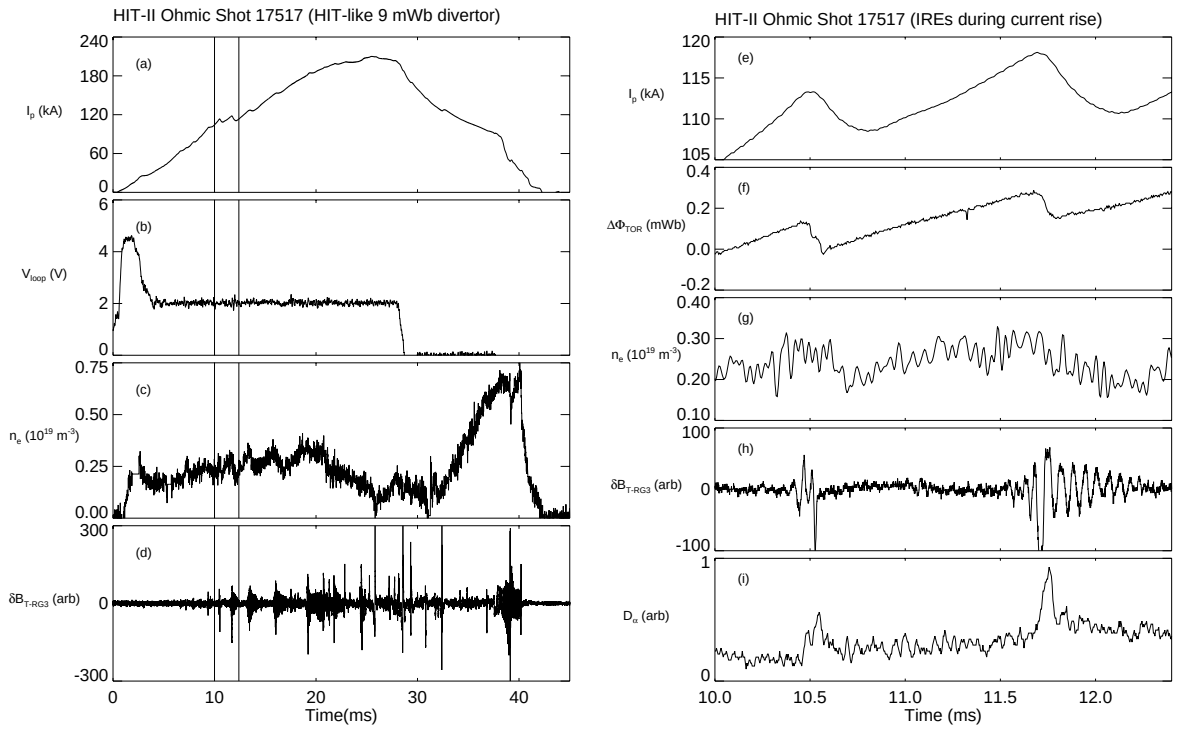

Figure 1. Examples of MHD events during the current rise. a) Plasma current, b) Loop voltage, c) Plasma density, and d) Edge toroidal field fluctuations at the mid-plane. Expanded time base for two MHD events: e) Plasma current, f) Diamagnetic flux, g) Plasma density, h) Edge toroidal field fluctuations at the mid-plane, and i) D_α line radiation. Observe a density drop after each event and a corresponding D_α burst.

slow response to changes in the plasma current. (The apparent rise time is 300μs - 400μs.) Internal Rowgoski segments around the toroidal perimeter at the mid-plane diagnostic gap measure the toroidal field fluctuations. They have a frequency response limited by the data rate of 1MHz. The diamagnetic loop response is also about 1MHz. The density is from a major chord of FIR interferometry passing nearly tangent to the magnetic axis. Figure 2 shows the MHD activity of an event in the decay phase of the discharge. Figure 3 shows the normalized poloidal field as a function of probe position along the outer shell before and after the MHD events of Figures 1 and 2. These data are from surface probes shown in Figure 9 of Reference [3]. The poloidal field is normalized to the mid-plane value. From equilibrium considerations it can be shown that a more hollow current profile has a greater natural elongation. Therefore, a relatively stronger poloidal field is required at the ends to contain the equilibrium inside the HIT-II shell. Thus, the higher normalized fields at the ends ($\pm 70^o$) in Figure 3 indicate a more hollow current profile.

Whether in the ramp-up or decay phase, these events can be described as global relaxation events which flatten the λ-profile ($\lambda \equiv \mu_0 j_\parallel / B$) while conserving helicity, causing a corresponding change in plasma elongation and major radius. Specifically, the ramp-up events redistribute the toroidal current from the edge plasma into the core region, thereby flattening a hollow current profile. Conversely, the decay events involve the movement of current density from the plasma core to the highly resistive, low-current edge, thereby

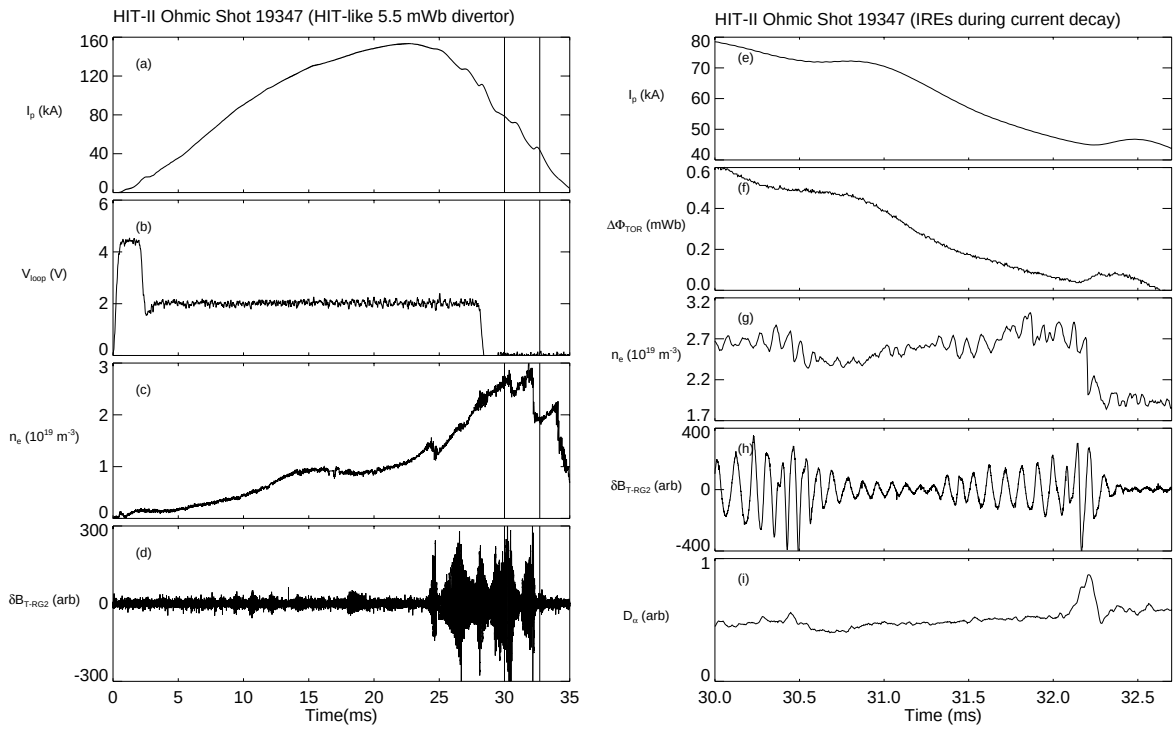

Figure 2. The same data as for Figure 1 but during the decay of a discharge. a) Plasma current, b) Loop voltage, c) Plasma density, and d) Edge toroidal field fluctuations at the mid-plane. Expanded time base for two MHD events: e) Plasma current, f) Diamagnetic flux, g) Plasma density, h) Edge toroidal field fluctuations at the mid-plane, and i) D_α line radiation. Observe a density drop after each event and a corresponding D_α burst

flattening a peaked current profile. The decay events observed in HIT-II are similar to the 'Internal Reconnection Events' (IRE's) that have been observed on other ST experiments, such as START [10,11].

3. Current drive mechanism

The rotating n=1 mode observed in HIT and HIT-II experiments is thought to be playing a role in the current drive mechanism for CHI. In HIT, the mode matched the plasma current drift in frequency (~50 kHz) and direction (for electrons), and large plasma currents (>150 kA) were never observed without mode activity [2]. In HIT-II, lower mode frequencies (~10 kHz) have been observed, and again the mode follows the electron current drift direction. This and other experimental results have led to the development of a new model for electromotive current drive, which has been named the electron locking model. In the model, magnetic relaxation is ascribed to the dynamo effect of a rotating saturated current-driven helical instability peaked on a mode resonant surface, in the presence of sheared magnetic profile. The electron fluid convects the distortion, since the Hall parameter $\omega_{ce}\tau_{ei}$ is very large. Electron fluid drift normal to the magnetic field occurs, in general, due to diamagnetism or to a radial electric field. This model could be applied to other devices with normal electron fluid drift. The E cross B drift is considered in applying the model to a CHI tokamak. Since the magnetic field is sheared, the electron drift velocities vary on different magnetic surfaces. Therefore, the saturated helical deformation itself becomes distorted by electron flux convection. Since the electron fluid drift velocity normal to the symmetric magnetic field on the mode resonant surface is in general largest on the mode resonant surface itself, the deformation is distorted by electron flux convection into a helically

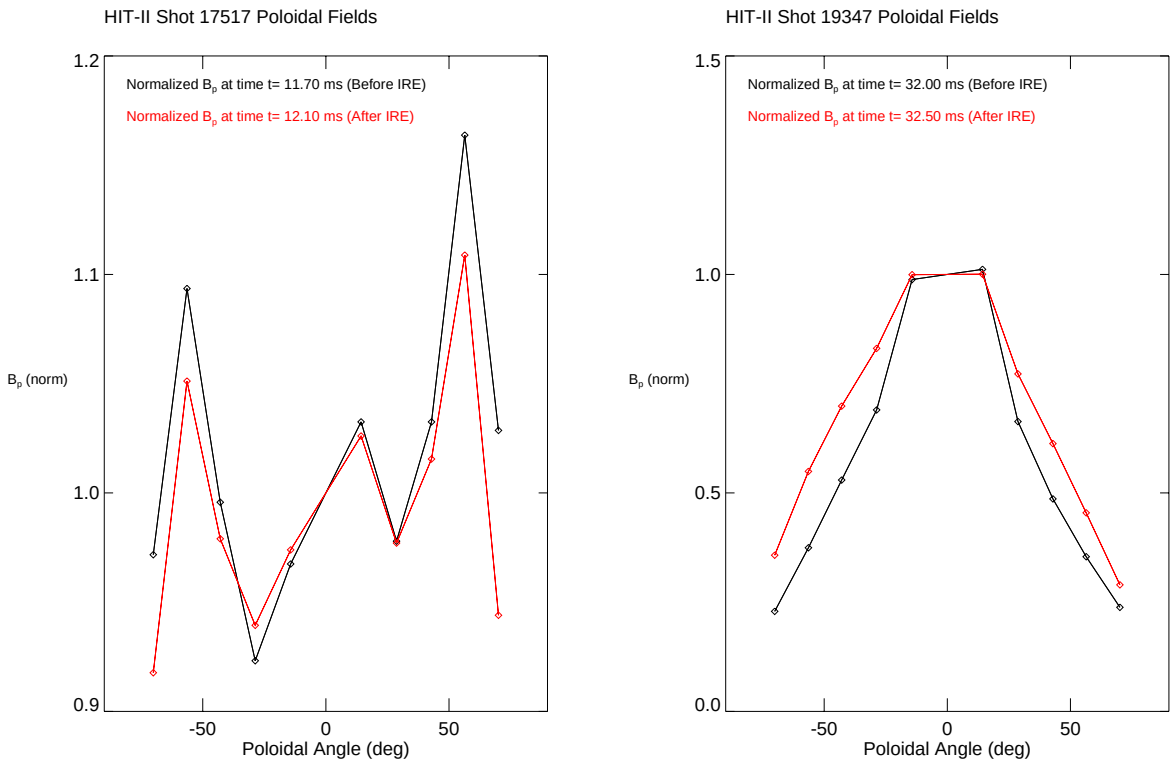

Figure 3. Normalized poloidal field at the outer shell before and after the IREs shown in the expanded time of Figures 1 and 2. The fields are normalized to the mid-plane value, which is at 0^o. The left frame is for an IRE during the rise in the current and the right is for a falling current.

antisymmetric shape. This means the mode is distinguishable from its reflection through a helical ribbon whose pitch matches the magnetic field line pitch on the mode resonant surface. Summarizing, the mode's helical antisymmetry is the result of differential electron fluid rotation. The helical sense of the mode's electromotive field is the same both inside and outside the mode resonant surface. Since the resonant surface is in a region of magnetic shear, both the helical magnetic field and the helical tangential current density switch sign at the resonant surface. Therefore, the resulting electromotive effect of the distortion is current drive interior to the mode resonant surface, and anti-current drive exterior to the mode resonant surface. The mode's electromotive effect occurs outside the mode separatrix, which defines magnetic islands, so that magnetic relaxation can occur apart from magnetic reconnection.

To test the electron locking model for a CHI tokamak, the HIT-II device is operated with different central column (CC) polarities, with the same flux boundary conditions, gas conditions, wall conditions, and sustainment bank timing. These experimental controls have been optimized for large plasma currents with low plasma density. Of course, in changing the CC from a cathode to an anode, the toroidal field current is reversed as well, to maintain the identity of the injector. The gas puff was the same for both CC polarities, except that the gas puff location was in the cathode for both cases.

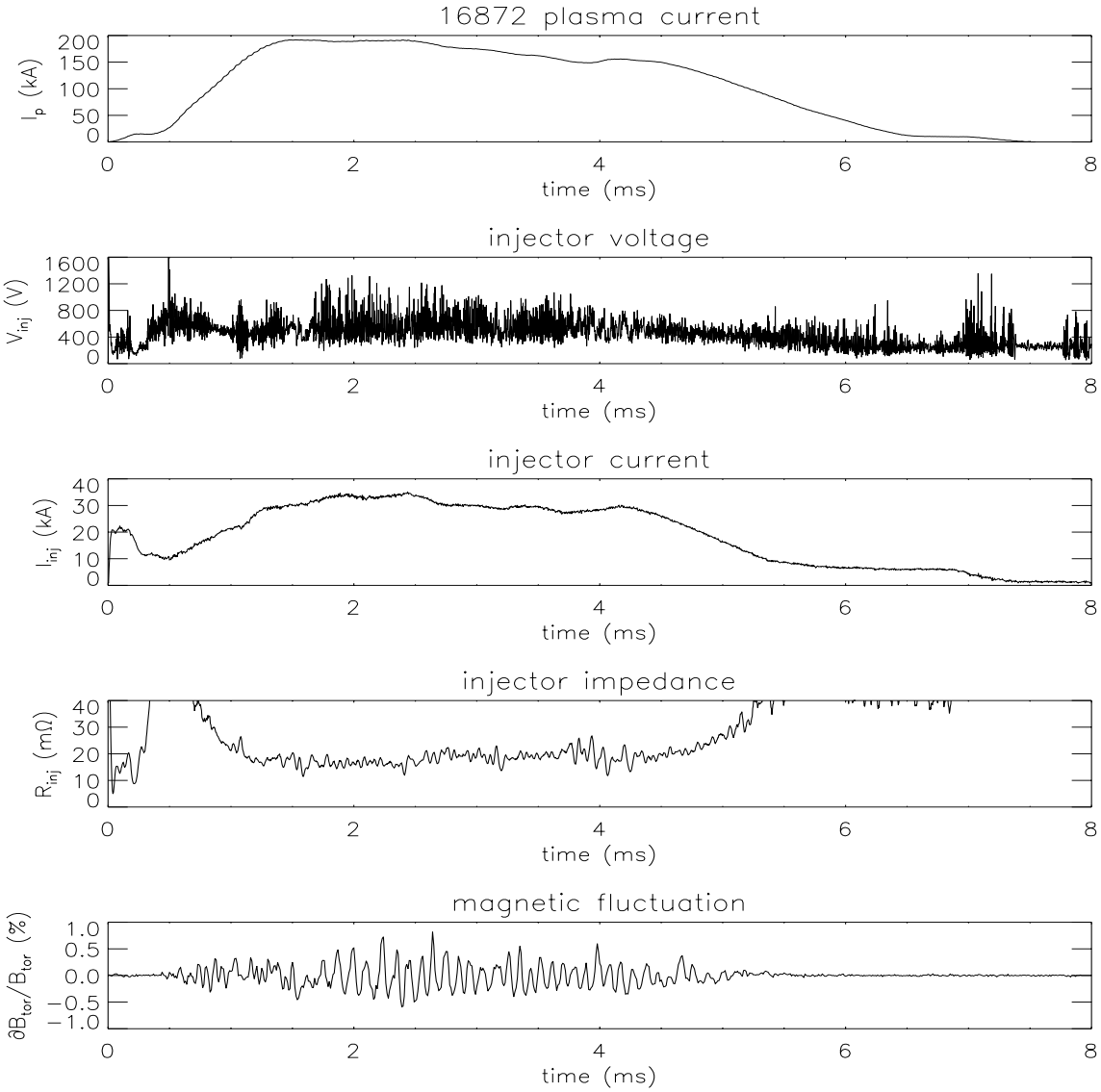

Figure 4. Plasma current, injector voltage, injector current, injector impedance, and edge toroidal field fluctuations normalized by the equilibrium value for a typical cathode CC discharge.

The results of these experiments show important differences between the two CC polarities. The direction of mode rotation matches the applied **E×B** in either case, which changes with CC polarity. Figure 4 shows key data for the normal cathode CC operation. Figure 5 shows similar data for the anode CC operation. Figure 6 shows the normalized poloidal field for the time indicated on four typical shots. Two are with cathode CC and two are with anode CC. A hollower profile is seen for anode CC. Figure 7 shows the toroidal rotation speed of CIII as a function of time for the two cases. In cathode CC operation the plasma is observed to rotate in the opposite direction as the plasma current but in anode CC it is in the same direction. The n=1 mode is common in cathode CC operation, but almost never observed with the anode CC, and when it does occur, it is only for a few cycles but at a higher frequency. Toroidal ion

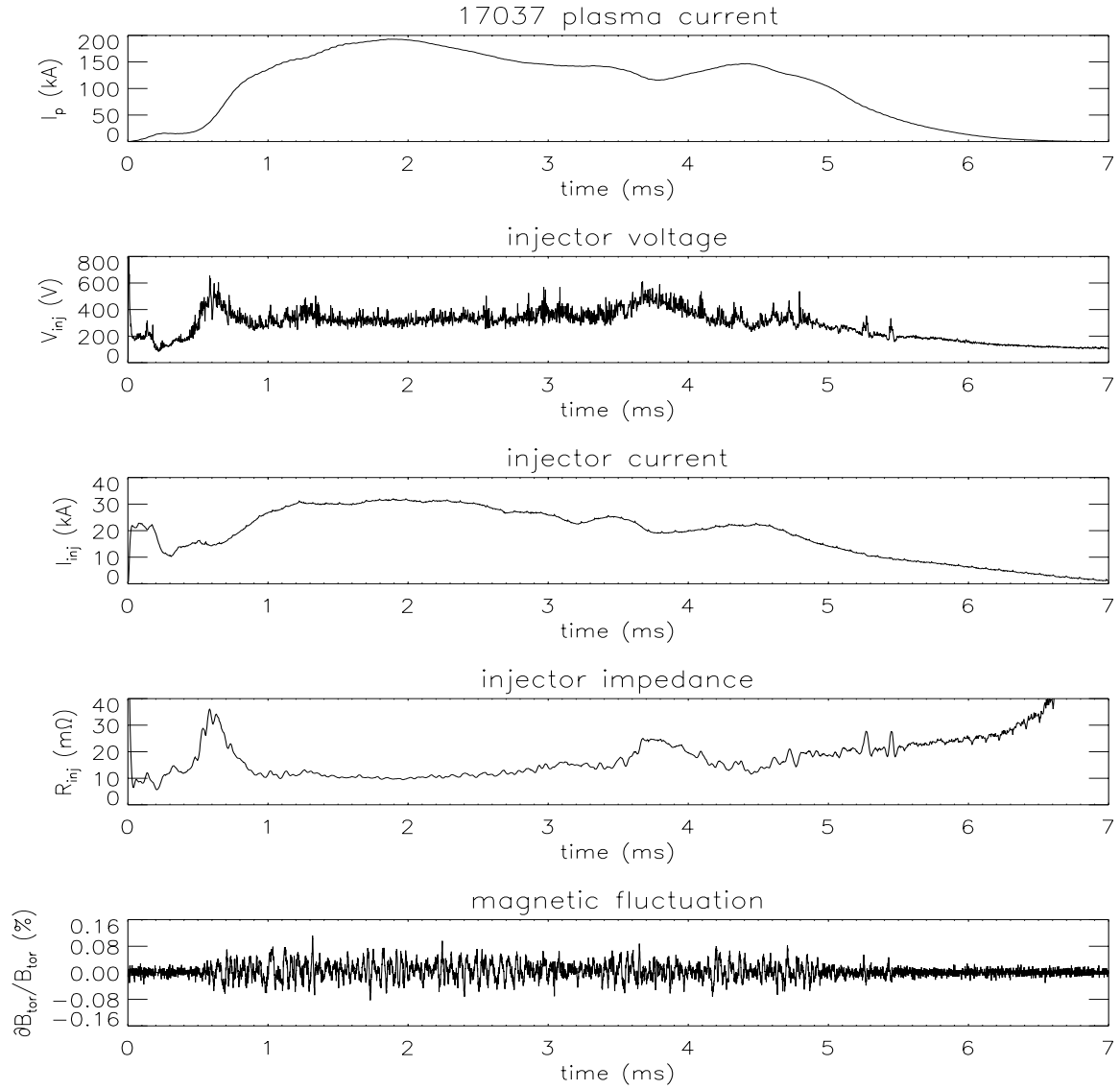

Figure 5. Plasma current, injector voltage, injector current, injector impedance, and edge toroidal field fluctuations normalized by the equilibrium value for a typical anode CC discharge.

flow is steady for cathode CC operation and suppressed for almost all anode CC pulses. The ion temperature profile, from OV ion Doppler data, shows is peaked at ~100 eV for cathode CC operation, while for anode CC it is flat and colder ~30 eV. Injector impedance is larger for cathode CC operation. These data are averages for time windows around the peak currents of 200 kA for both polarities.

Each of these results is consistent with the predictions of the electron locking model. For a hollow CHI profile with cathode CC polarity the predicted mode activity results in current drive interior to the mode resonant surface and anti-current drive exterior to the mode resonant surface, at the outboard edge, where the mode amplitude is largest. This tends to

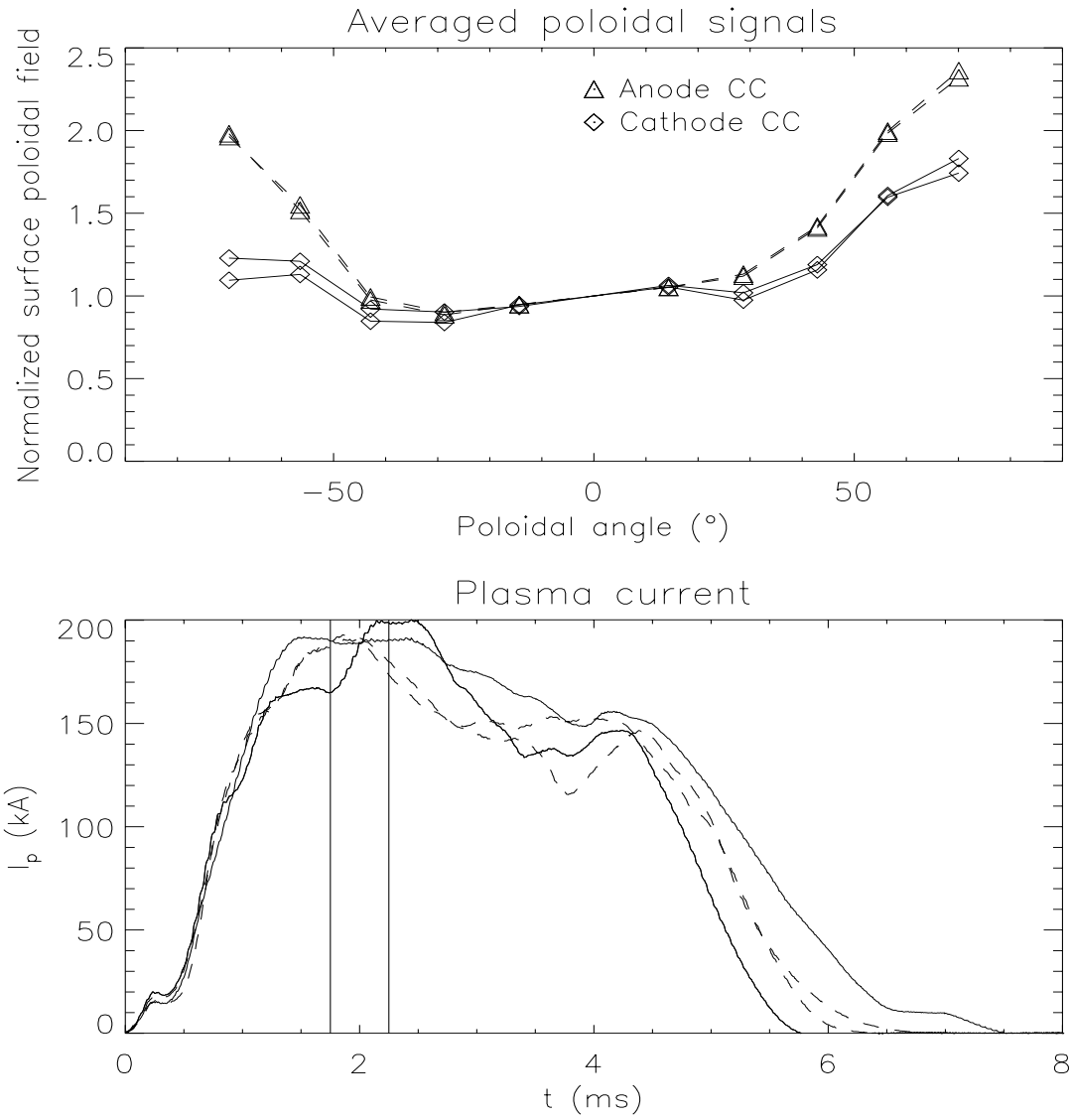

Figure 6. Normalized edge poloidal field for two cathode CC and two anode CC discharges and the plasma current verse time for all four discharges. The vertical lines show the time over which the data was averaged to obtain the fields of the upper frame.

flatten the hollow current profile, as the source of the current-driven instability is the radial variation of current density. The electromotive activity results in higher injector impedance and more ion heating. Electromotive current drive inside the resonant surface also results in toroidal ion spinup, which tends to cancel the plasma current. Meanwhile, for anode CC polarity, the effect of mode activity near the outboard edge is anti-current drive interior to the mode resonant surface and current drive exterior to the mode resonant surface. Since this activity tends to make the hollow profile more hollow, there is generally less free energy available for the instability, and its amplitude is therefore smaller. Likewise, lower injector impedance and less ion heating occur. When the mode does occur in anode CC polarity, during the initial current rise portion of the discharge, its frequency is larger, which implies that the edge region with radial electric field responsible for mode rotation is thinner, also consistent with the more hollow profile. When ion flow does occur for anode CC polarity, it is in the same direction as the plasma current, which implies that ion spinup is tending to

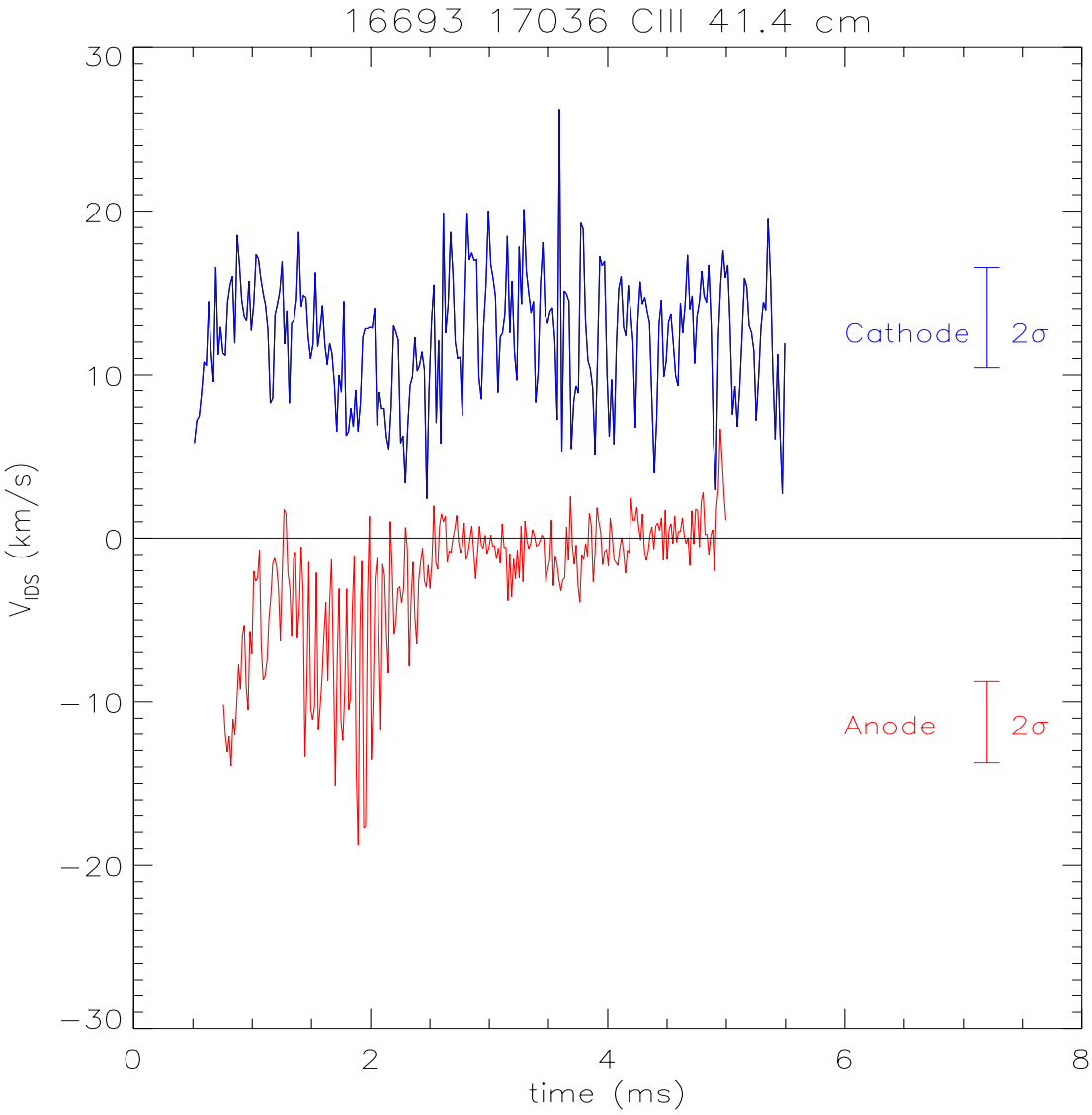

Figure 7. CIII velocity in the toroidal direction measured by Doppler spectroscopy. The upper curve is for cathode CC and the lower is for anode CC. The impact parameter, in major radius, is 0.4 m. Positive ion velocity is in the opposite direction of the plasma current.

cancel the electromotive anti-current drive inside the mode resonant surface. Summarizing, the electron locking model accounts for each of the important differences between cathode CC and anode CC operation in the CHI tokamak.

4. Double separatrix operation

Figure 8 shows a new flux configuration being used on HIT-II. A weak divertor is formed near the absorber insulator. (The absorber insulator is at the top in Figure 8. It is call the absorber because **E**×**B** is into this insulator.) When the equilibrium is formed a thin currentless region is formed next to the walls. The injector current is driven on the flux between the X-point at the absorber and the X-point at the injector. This double separatrix configuration gives less shorting parasitic current in the flux absorbing region, much better reproducibility, lower impurity radiation with more relative power from higher charge states, more current amplification, the n=1 is consistently observed, and the n=1 is at a higher frequency. The injector current is nearly constant in time even though the voltage is changing

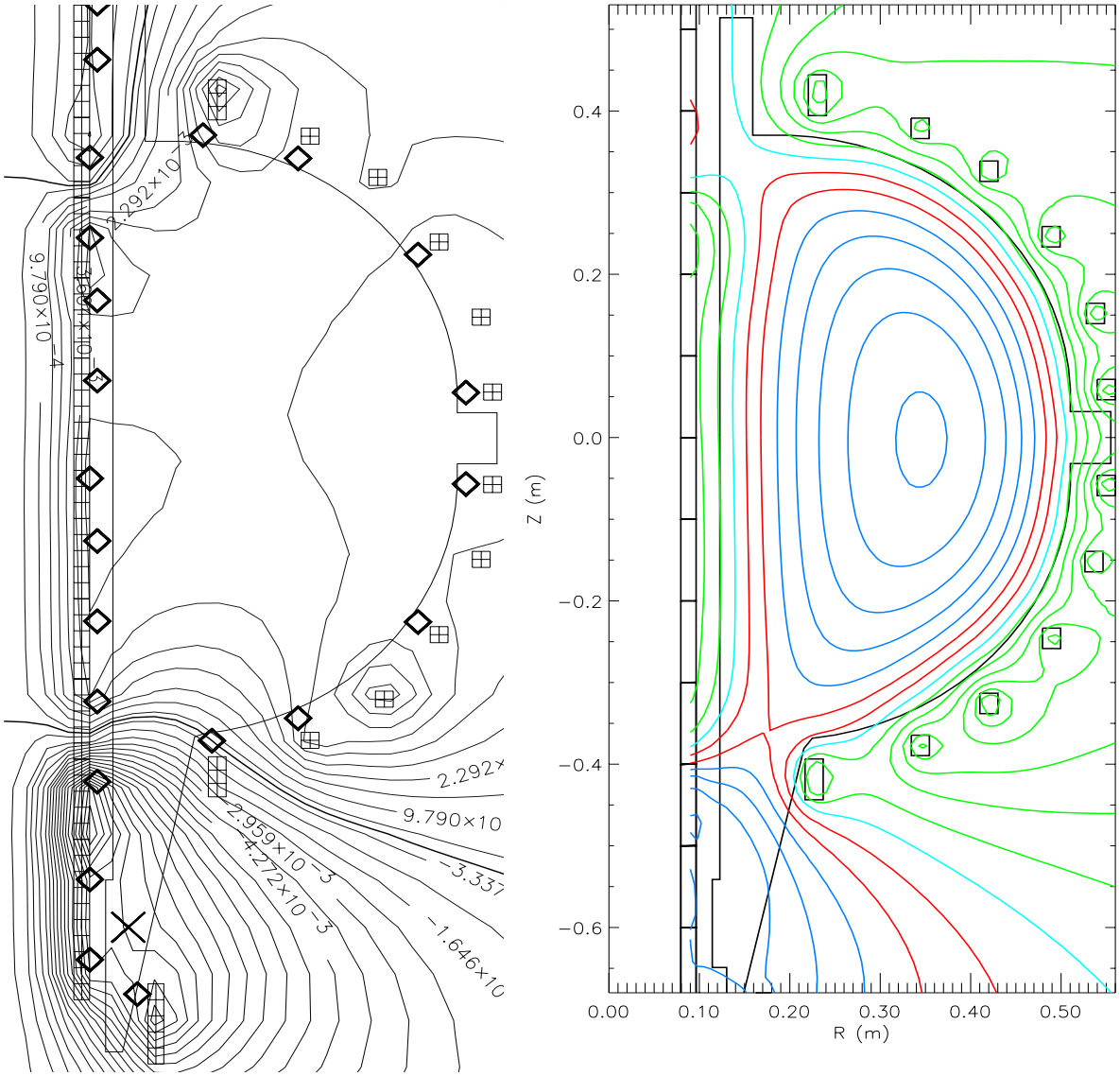

Figure 8. Double separatrix configuration. The left frame is the vacuum flux. the right frame is an EFIT reconstruction of the equilibrium during CHI discharge #19205.

and the value of the current is adjusted only by changing the injector flux, consistent with earlier predictions of injector impedance [1]. Using the new configuration CHI experiments have achieved reduced plasma density to the low 10^{19} m^{-3} level, compatible with Ohmic operations. This has involved reducing the gas puff for CHI pulses from more than 800 mTorr-liters to less than 120 mTorr-liters. In this low-density regime, the CHI plasmas also exhibited good repeatability. Figure 9a-d shows the time history of plasma parameters for the 150kA discharge use for the EFIT plot of Figure 8. For this discharge the injector flux is 10mWb. Figure 9e-h shows a lower current discharge with the injector flux at 5.5mWb. The discharge is longer lived because the lower injector current discharges the capacitor bank more slowly. Note, the plasma current has a correlation with the injector voltage while the injector current is fairly constant. This indicates that the plasma current depends somewhat on helicity injection and is not just from the geometric wrap up of the injector current on open field lines. Figure 9e-h also shows the effect of adding transformer action to these new CHI discharges. At 10ms into the discharge a 2V loop voltage is added on top of the CHI discharge. The main effect is that the time of the discharge is extended an additional 5ms.

Even though the loop voltage is on for 10ms the plasma current stops as the CHI current drive shuts off.

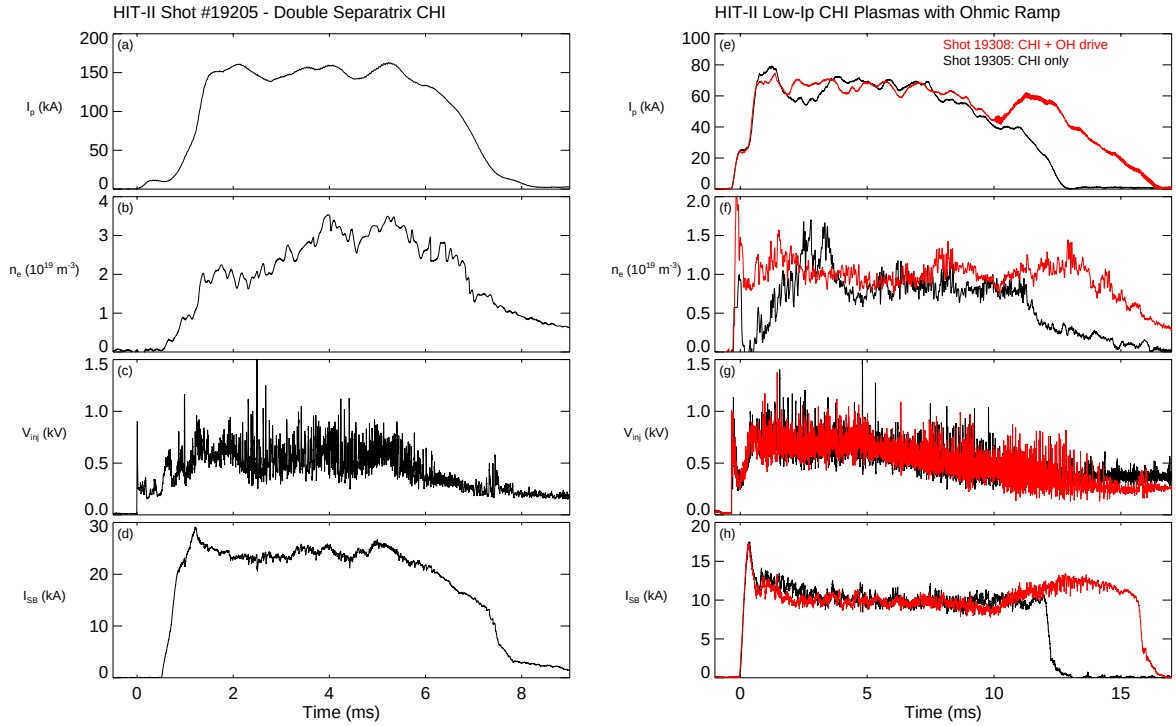

Figure 9. Time dependence of parameters during two double separatrix discharges. Frames a-d show the plasma current, density, injector voltage, and injector current for a 150kA CHI discharge. Frames e-h show the same parameters for a lower current CHI discharge. The red traces are of a lower current CHI discharge with a two volt loop voltage added from 10ms to 20ms.

References:

[1] T. R. Jarboe, Fusion Technology **15**, 7 (1989).
[2] B. A. Nelson *et al.*, Phys. Plasmas **2**, 2337 (1995).
[3]T. R. Jarboe *et al.*, Phys. Plasmas **5**, 1807 (1998)
[4] N. Fisch, Rev. Mod. Phys. **59**, 175 (1987).
[5] A. H. Boozer, Phys. Fluids **31**, 591 (1988)
[6] T. R. Jarboe, Plasma Phys. Control. Fusion **36**, 945 (1994).
[7] J. B. Taylor, Rev. Mod. Phys. **58**, 741 (1986)
[8] M. Ono, Phys. Rev. Lett. **59**, 2165 (1987)
[9] A. Sykes et al, "The START Spherical Tokamak", Proceedings of the Fifteenth IAIA conference on Plasma Physics and Controlled Fusion, Seville Spain, 1994.
[10]: T. C. Hender *et al.*, Phys. Plas. **6**, 1999, pp. 1958-1968.
[11]: R. J. Buttery *et al.*, Proceedings of the 1996 EPS Conference on Controlled Fusion, vol. I, p. 416.